Full paper

Applied Organometallic Chemistry

Received: 20 January 2015 Revised: 8 April 2015 Accepted: 12 April 2015 Published online in Wiley Online Library: 25 May 2015

(wileyonlinelibrary.com) DOI 10.1002/aoc.3330

Incorporation of azo group at axial position of silatranes: synthesis, characterization and antimicrobial activity

Gurjaspreet Singh[a]*, Amandeep Saroa[a], Shally Girdhar[a], Sunita Rani[a], Duane Choquesillo-Lazarte[b]* and Subash Chandra Sahoo[a]

4-Aminoazobenzene-derived silatranes bearing urea and aminosuccinimide as linker groups at the axial position are reported. The urea functionality is introduced in a silane (2) by the rearrangement reaction between 3-isocyanatopropyltriethoxysilane and 4-aminoazobenzene. *N*-(3-silatranylpropyl)-*N*′-[(*p*-phenyldiazenyl)phenyl]urea and *N*-[3-(3,7,10-trimethylsilatranyl)propyl]-*N*′-[(*p*-phenyldiazene)phenyl]urea were prepared by transesterification reaction of 2 with triethanolamine and trisisopropanolamine, respectively. An efficient method for C–N bond formation is described for the synthesis of 3-(silatranylpropyl)amino-*N*-[(*p*-phenyldiazene)phenyl]pyrrolidine-2,5-dione and 3-[(3,7,10-trimethylsilatranyl)propyl]amino-*N*-[(*p*-phenyldiazene)phenyl]pyrrolidine-2,5-dione via aza-Michael addition reaction of aminopropylsilatranes with 4-(*N*-maleimido) azobenzene under mild conditions. All the compounds were well characterized using elemental analysis, spectroscopic techniques, thermogravimetric analysis and X-ray diffraction. UV–visible spectroscopy indicates that the 4-aminoazobenzene-derived silatranes are capable acetate receptors. The synthesized compounds were screened for possible antimicrobial properties with the results showing a modest activity. Copyright © 2015 John Wiley & Sons, Ltd.

Additional supporting information may be found in the online version of this article at the publisher's web-site.

Keywords: 4-aminoazobenzene; silatrane; urea; aminosuccinimide; acetate receptor; antimicrobial activity

Introduction

Azo dyes are a well-known family of organic dyes, which are widely used in diverse areas such as dyes, nonlinear optical chromophores, photoresponsive molecular switches, pH indicators and photostorage units.[1–6] Along with their conventional roles in industrial applications, azo dyes are known to take part in a number of biological reactions such as inhibition of DNA and RNA and biological activities against bacteria and fungi.[7,8] Recently, metal complexes of dyes have attracted much attention in both academic and applied research due to their interesting electronic and geometric features.[9,10] To the best of our knowledge, only a handful of compounds have demonstrated successful incorporation of azo dyes into axial position of silatranes. The reason for choosing silatranes over numerous other metal complexes is the structural aspect of silatranes, especially the N→Si transannular bond in distorted trigonal bipyramidal geometry at the silicon atom.[11] These modified compounds are significant because of the stereoelectronic effect of the silatranyl group in shaping the reactivity of exocyclic functional groups apical to the transannular bond.[12] Silatranes have a wide range of geometries depending upon these axial groups which enhance an array of biological and material science applications.[13] Contemporary chemists have boosted work on the modification of exocyclic functional groups due to enhanced biological and material science applications of modified silatranes.[14]

To incorporate azo groups at axial positions of silatranes, two routes were pursued in the work reported in this paper. In the first route, derivatization of 4-aminoazobenzene (**1**) was carried out by the reaction with 3-isocyanatopropyltriethoxysilane which led to the synthesis of a non-symmetric urea-substituted silane (**2**). These substituted urea-trialkoxysilanes have attracted considerable attention due to applications in nonlinear optical chromophores, hybrid materials and functionalized mesoporous silicas.[15,16] In the second route, 4-(*N*-maleimido)azobenzene (**7**) acting as a strong electron-accepting moiety was incorporated at the axial position of aminopropylsilatranes (**5**, **6**) by an aza-Michael addition reaction. These types of compounds are attractive for chemists working in the field of biomimetic chemistry as new supple receptors for amines.[17,18] So in the work reported in this article, we integrated silatranes with azobenzene at the axial position using urea and aminosuccinimide as linker groups which might lead to the generation of new materials. Both urea and aminosuccinimide groups are valuable for making 4-aminoazobenzene-derived silatranes as anion receptors for acetate groups via hydrogen-bonding interactions. These interactions are easily monitored using anion-complexation-induced charge transfer bands in UV–visible absorption spectra. Due to a wide range of biological properties

* *Correspondence to: Gurjaspreet Singh, Department of Chemistry, Panjab University, Chandigarh 160014, India. E-mail: gjpsingh@pu.ac.in*

* *Duane Choquesillo-Lazarte, Laboratorio de Estudios Cristalográficos, IACT, CSIC-University of Granada, Avenida de las Palmeras 4, 18100, Armilla (Granada), Spain. E-mail: duanec@ugr.es*

a *Department of Chemistry, Panjab University, Chandigarh 160014, India*

b *Laboratorio de Estudios Cristalográficos, IACT, CSIC-University of Granada, Avenida de las Palmeras 4, 18100, Armilla (Granada), Spain*

of silatranes, such as antimicrobial, antifungal and antitumor activities,[19] we studied the antimicrobial properties of all the synthesized silatranes (**3**, **4**, **8** and **9**) against reference microorganisms.

Materials and methods

Synthesis and characterization

3-Isocyanatopropyltriethoxysilane, 3-aminopropyltriethoxysilane, triethanolamine, trisisopropanolamine and maleic anhydride were purchased from Sigma-Aldrich. Compound **1**,[20] aminopropylsilatranes **5** and **6**[21] and **7**[22] were prepared as reported in the literature. All reactions were performed under nitrogen atmosphere. ^{1}H NMR and ^{13}C NMR spectra were recorded in $CDCl_3$ solution using 400 MHz (Bruker Avance AL 400) and 300 MHz (JEOL AL 300) FT NMR instruments. Infrared spectra were obtained with a Thermo Nicolet Nexus 670 spectrometer. C, H and N analyses were performed with a FLASH-2000 organic element analyser while Si content was estimated gravimetrically. Mass spectral measurements (ESI source with capillary voltage of 2500 V) were carried out with a VG Analytical (70-S) spectrometer. Thermal analysis was conducted using an SDT Q 600V20.9 Build 20TGA instrument. A weighed amount of sample was loaded in alumina pans and ramped at 10°C min^{-1} to 800°C in dry air at 60 ml min^{-1}. UV–visible spectra were recorded with a Varian Cary 500 spectrophotometer.

X-ray crystallography

Crystals for measurement were prepared under inert conditions immersed in perfluoropolyether as protecting oil for manipulation. Suitable crystals were mounted on MiTeGenMicromounts™ and these samples were used for data collection. The data were collected with a Bruker D8 Venture (100 K) diffractometer. The data were processed with the APEX2 program[23] and corrected for absorption using SADABS.[24] The structures were solved by direct methods, which revealed the position of all non-hydrogen atoms. These atoms were refined on F^2 by a full-matrix least-squares procedure using anisotropic displacement parameters.[25] All hydrogen atoms were located in different Fourier maps and included as fixed contributions riding on attached atoms with isotropic thermal displacement parameters 1.2 times those of the respective atom. The geometric calculations were carried out with PLATON[26] and drawings were produced with Olex2[27] and MERCURY.[28] Additional crystal data and more information about the X-ray structural analyses are given in Tables 1 and 2.

Minimal inhibitory concentration (MIC) measurement

The antimicrobial activity of compounds was checked using the broth microdilution method in a 96-well microtitre plate.[29] Growth medium (100 µl) was added in each well except the first, in which 200 µl of stock solution (800 µg ml^{-1}) of test compound in dimethylsulfoxide was added. After appropriate mixing, twofold serial dilutions were made ranging from 0.78 to 400 µl ml^{-1}. Actively growing bacterial culture (100 µl) containing 1×10^5 cells was added to all the dilutions and mixed gently. The plates were incubated at 37°C for 18 h. The MIC of the given compounds was measured as the maximum dilution of compound showing no visible growth of bacteria.

Table 1. Crystal data and structure refinement for compounds **2** and **9**

	2	9
Empirical formula	$C_{22}H_{32}N_4O_4Si$	$C_{28}H_{37}N_5O_5Si$
Formula weight	444.61	551.72
T (K)	100	100
λ (Å)	1.54178	1.54178
Crystal system	Monoclinic	Monoclinic
Space group	$P2_1/c$	$C2/c$
Unit cell dimensions		
a (Å)	15.2270(4)	30.358(3)
b (Å)	9.2457(2)	8.4632(6)
c (Å)	18.4518(5)	25.907(2)
α (°)	90	90
β (°)	114.2300(11)	119.618(5)
γ (°)	90	90
Volume (Å^3)	2368.88(10)	5786.3(9)
Z	4	8
D (calcd; g cm^{-3})	1.247	1.267
Absorption coefficient (mm^{-1})	1.161	1.092
F (000)	952	2352
Theta range for data collection (°)	3.18–66.75	3.35–66.56
Reflections collected	15 176	20 567
Independent reflections	4122 (R(int) = 0.0246)	4988 (R(int) = 0.0801)
Data / restraints / parameters	4122 / 0 / 283	4988 / 0 / 383
Goodness-of-fit on F^2	1.058	1.058
Final R indices ($I > 2\sigma(I)$)	$R_1 = 0.0559$, $wR_2 = 0.1437$	$R_1 = 0.0755$, $wR_2 = 0.1894$
R indices (all data)	$R_1 = 0.0609$, $wR_2 = 0.1483$	$R_1 = 0.0926$, $wR_2 = 0.2041$
Largest diff. peak and hole (eÅ^{-3})	0.908 and −0.489	0.871 and −0.665

Table 2. Selected bond lengths (Å) and angles (°) for **2** and **9**

Compound **2**		Compound **9**	
Si(1)–O(2)	1.6238(19)	Si(1)–O(1)	1.666(2)
Si(1)–O(1)	1.6269(18)	Si(1)–O(2)	1.661(2)
Si(1)–O(3)	1.6092(19)	Si(1)–O(3)	1.658(2)
Si(1)–C(7)	1.845(2)	Si(1)–N(1)	2.248(3)
O(2)–Si(1)–O(1)	111.69(11)	Si(1)–C(10)	1.878(3)
O(2)–Si(1)–C(7)	104.18(10)	O(1)–Si(1)–C(10)	97.92(12)
O(1)–Si(1)–C(7)	111.87(10)	O(2)–Si(1)–O(1)	121.04(13)
O(3)–Si(1)–O(2)	108.61(11)	O(2)–Si(1)–N(1)	80.90(11)
O(3)–Si(1)–O(1)	106.27(10)	O(2)–Si(1)–C(10)	95.50(13)
		O(3)–Si(1)–O(1)	115.02(13)
		O(3)–Si(1)–O(2)	117.70(12)
		O(3)–Si(1)–N(1)	82.25(11)
		O(3)–Si(1)–C(10)	101.83(13)
		C(10)–Si(1)–N(1)	175.53(13)

Syntheses

*Synthesis of N-(3-triethoxysilylpropyl)-N′-[(p-phenyldiazenyl)phenyl]urea (**2**)*

3-Isocyanatopropyltriethoxysilane (2.00 g, 8.06 mmol) was added dropwise to a stirred solution of **1** (1.59 g, 8.06 mmol) in chloroform. The resulting mixture was refluxed at 70°C for 4 h. Then the solvent was evaporated under vacuum to afford a dark orange-coloured solution of **2** that eventually solidified at room temperature on resting for 15 min. Silane **2** was highly hygroscopic and its crystals were grown in tetrahydrofuran.

Yield 2.93 g (82%); m.p. 77–79°C. Anal. Calcd for $C_{22}H_{32}N_4O_4Si$ (444) (%): C, 59.45; H, 7.20; N, 12.61; Si, 6.30. Found (%): C, 58.80; H, 7.76; N, 12.49; Si, 6.16. IR (cm^{-1}): 1074, 1511, 1558, 1648, 2888, 2933, 3346. ^1H NMR (400 MHz, $CDCl_3$, δ, ppm): 0.59 (t, 2H, $J = 8.2$ Hz, $H^{16A,16B}$), 1.16 (t, 9H, $J = 6.9$ Hz, CH_3), 1.60 (m, 2H, $H^{15A,15B}$), 3.64 (m, 2H, $H^{14A,14B}$), 3.74 (q, 6H, $J = 6.9$ Hz, OCH_2), 5.35 (s, 1H, NHC^{14}), 7.09 (s, 1H, NHC^{12}), 7.33–7.81 (m, 9H, Ar–H). ^{13}C NMR (75 MHz, $CDCl_3$, δ, ppm): 7.82 (C^{16}), 18.45 (CH_3), 23.66 (C^{15}), 54.33 (C^{14}), 58.49 (OCH_2), 119.23 ($C^{9,11}$), 122.88 ($C^{8,12}$), 122.89 ($C^{2,6}$), 128.93 ($C^{3,5}$), 130.33 (C^4), 142.05 (C^{10}), 152.69 (C^1), 152.78 (C^7), 155.62 (C^{13}). MS, *m/z* (relative abundance (%), assignment): 444 (25.1, M^+).

*Synthesis of N-(3-silatranylpropyl)-N′-[(p-phenyldiazenyl)phenyl]urea (**3**)*

A two-necked round-bottomed flask fitted with a magnetic stirrer and Dean–Stark apparatus was sequentially charged in a stream of nitrogen with silane **2** (1.20 g, 2.70 mmol) dissolved in 30 ml of dry toluene. The tripodal ligand triethanolamine (0.36 g, 2.70 mmol) was added slowly to the solution and allowed to stir at 25°C for 10 min in the presence of catalytic amount of sodium ethoxide. The mixture was refluxed for 4 h and the solvent was removed under reduced pressure to afford an orange-coloured product with anhydrous hexane.

Yield 1.03 g (85%); m.p. 186–188°C. Anal. Calcd for $C_{22}H_{29}N_5O_4Si$ (455) (%): C, 58.02; H, 6.37; N, 15.38; Si, 6.15. Found (%): C, 58.17; H, 6.25; N, 15.12; Si, 6.03. IR (cm^{-1}): 583, 679, 1100, 1559, 1597, 1658, 2876, 2929, 3329. ^1H NMR (400 MHz, $CDCl_3$, δ, ppm): 0.42 (t, 2H, $J = 8.2$ Hz, $H^{16A,16B}$), 1.61 (m, 2H, $H^{15A,15B}$), 2.72 (t, 6H, $J = 5.8$ Hz, CH_2N), 3.20 (m, 2H, $H^{14A,14B}$), 3.68 (t, 6H, $J = 5.8$ Hz, OCH_2), 6.87 (s, 1H, NHC^{14}), 7.37 (s, 1H, NHC^{10}), 7.35–7.81 (m, 9H, Ar–H). ^{13}C NMR (100.6 MHz, $CDCl_3$, δ, ppm): 14.07 (C^{16}), 24.42 (C^{15}), 47.05 (C^{14}), 50.08 (NCH_2), 58.75 (OCH_2), 119.03 ($C^{9,11}$), 122.47 ($C^{8,12}$), 123.37 ($C^{2,6}$), 128.30 ($C^{3,5}$), 128.50 (C^4), 142.33 (C^{10}), 151.47 (C^1), 151.54 (C^7), 155.63 (C^{13}). MS, *m/z* (relative abundance (%), assignment): 456 (100, $(M+H)^+$), 477 (49.1, $(M+Na)^+$), 493 (8.2, $(M+K)^+$), 932 (72.4, $(2M+Na)^+$).

*Synthesis of N-[3-(3,7,10-trimethylsilatranyl)propyl]-N′-[(p-phenyldiazenyl)phenyl]urea (**4**)*

Compound **4** was synthesized using a method similar to that for **3**, with trisisopropanolamine being used as a tripodal ligand instead of triethanolamine.

Yield 1.07 g (81%); m.p. 197–199°C. Anal. Calcd for $C_{25}H_{35}N_5O_4Si$ (497) (%): C, 60.36; H, 7.04; N, 15.09; Si, 5.63. Found (%): C, 60.28; H, 6.97; N, 14.94; Si, 5.51. IR (cm^{-1}): 544, 695, 1064, 1108, 1538, 1597, 1662, 2868, 2937, 3346. ^1H NMR (400 MHz, $CDCl_3$, δ, ppm): 0.42 (t, 2H, $J = 8.2$ Hz, $H^{16A,16B}$), 1.13 (m, 9H, CH_3), 1.62 (m, 2H, $H^{15A,15B}$), 2.73 (m, 6H, CH_2N), 3.19 (m, 2H, $H^{14A,14B}$), 3.83 (m, 3H, OCH), 5.63 (s, 1H, NHC^{14}), 7.35–7.81 (m, 9H, Ar–H), 7.68 (s, 1H, NHC^{10}). ^{13}C NMR (75 MHz, $CDCl_3$, δ, ppm): 15.29 (C^{16}), 20.33, 20.42, 20.77 (CH_3), 25.16 (C^{15}), 42.84 (C^{14}), 61.73, 62.04, 63.40 (NCH_2), 65.00, 65.16, 65.79 (OCH), 118.41 ($C^{9,11}$), 122.60 ($C^{8,12}$), 124.17 ($C^{2,6}$), 128.87 ($C^{3,5}$), 130.05 (C^4), 143.30 (C^{10}), 151.74 (C^1), 151.89 (C^7), 155.70 (C^{13}). MS, *m/z* (relative abundance (%), assignment): 498 (100, $(M+H)^+$), 520 (33.9, $(M+Na)^+$), 536 (7.4, $(M+K)^+$), 1017 (9.1, $(2M+Na)^+$).

*Synthesis of 3-(silatranylpropyl)amino-N-[(p-phenyldiazenyl)phenyl]-pyrrolidine-2,5-dione (**8**)*

In a 100 ml two-neck round-bottom flask, **7** (1.20 g, 4.31 mmol) was dissolved in 50 ml of chloroform under nitrogen atmosphere. A solution of 3-aminopropylsilatrane **5** (1.00 g, 4.31 mmol) in chloroform was added dropwise and the mixture was stirred for 10 h at room temperature. The solvent was evaporated under reduced pressure and an orange-coloured viscous oil was obtained. Upon addition of dry hexane, an orange–red solid was extracted.

Yield 1.64 g (74%); m.p. 201–203°C. Anal. Calcd for $C_{25}H_{31}N_5O_5Si$ (509) (%): C, 58.93; H, 6.09; N, 13.75; Si, 5.50. Found (%): C, 58.76; H, 6.32; N, 13.67; Si, 5.38. IR (cm^{-1}): 548, 687, 1097, 1118, 1397, 1552, 1605, 1710, 2880, 2933, 3288. ^1H NMR (400 MHz, $CDCl_3$, δ, ppm): 0.46 (t, 2H, $J = 8.2$ Hz, $H^{19A,19B}$), 1.66 (m, 2H, $H^{18A,18B}$), 2.16 (s, 1H, NH), 2.64 (m, 2H, $H^{17A,17B}$), 2.74 (m, 1H, H^{15A}), 2.80 (t, 6H, $J = 5.8$ Hz, CH_2N), 3.09 (dd, 1H, $J = 8.3$, 18.0 Hz, H^{15B}), 3.75 (t, 6H, $J = 5.8$ Hz, OCH_2), 3.97 (dd, 1H, $J = 5.0$, 8.3 Hz, H^{16}), 7.43–8.02 (m, 9H, Ar–H). ^{13}C NMR (75.5 MHz, $CDCl_3$, δ, ppm): 13.20 (C^{19}), 24.76 (C^{18}), 36.66 (C^{15}), 50.59 (C^{17}), 51.30 (NCH_2), 56.23 (C^{16}), 57.92 (OCH_2), 123.21 ($C^{9,11}$), 123.53 ($C^{8,12}$), 124.06 ($C^{2,6}$), 129.07 ($C^{3,5}$), 131.18 (C^4), 142.73 (C^{10}), 151.80 (C^1), 151.92 (C^7), 173.93 (C^{13}), 176.68 (^{14}). MS, *m/z* (relative abundance (%), assignment): 510 (100, $(M+H)^+$).

*Synthesis of 3-[(3,7,10-trimethylsilatranyl)propyl]amino-N-[(p-phenyldiazene)phenyl]pyrrolidine-2,5-dione (**9**)*

Compound **9** was prepared using a method similar to that for **8**, with 3,7,10-trimethyl-substituted silatrane **6** being used instead of silatrane **5**. Crystals of **9** were grown in chloroform solution by slow evaporation.

Yield 1.59 g (79%); m.p.: 209–211°C. Anal. Calcd for $C_{28}H_{37}N_5O_5Si$ (551) (%): C, 60.98; H, 6.71; N, 12.70; Si, 5.08. Found (%): C, 60.15; H, 6.56; N, 12.59; Si, 4.98. IR (cm^{-1}): 547, 692, 1061, 1149, 1384, 1544, 1601, 1710, 2892, 2937, 3305. ^1H NMR (400 MHz, $CDCl_3$, δ, ppm): 0.48 (t, 2H, $J = 8.2$ Hz, $H^{19A,19B}$), 1.19 (m, 9H, CH_3), 1.69 (m, 2H, $H^{18A,18B}$), 2.21 (s, 1H, NH), 2.72 (m, 2H, $H^{17A,17B}$), 2.78 (m, 1H, H^{15A}), 2.80 (m, 6H, CH_2N), 2.99 (dd, 1H, $J = 8.3$, 18.0 Hz, H^{15B}), 3.92 (m, 3H, OCH), 4.10 (dd, 1H, $J = 5.0$, 8.3 Hz, H^{16}), 7.46–8.03 (m, 9H, Ar–H). ^{13}C NMR (75.5 MHz, $CDCl_3$, δ, ppm): 13.27 (C^{19}), 20.41, 20.51, 20.92

(CH_3), 24.93 (C^{18}), 36.69 (C^{15}), 50.52 (C^{17}), 56.26 (C^{16}), 61.92, 62.43, 63.50 (NCH_2), 65.14, 65.33, 65.57 (OCH), 123.24 ($C^{9,11}$), 123.55 ($C^{8,12}$), 124.48 ($C^{2,6}$), 129.27 ($C^{3,5}$), 131.22 (C^4), 142.80 (C^{10}), 151.76 (C^1), 151.81 (C^7), 173.84 (C^{13}), 176.58 (^{14}). MS, *m/z* (relative abundance (%), assignment): 552 (100, $(M+H)^+$).

Results and discussion

Synthesis

The non-symmetric urea-substituted silane **2** was synthesized by the rearrangement reaction of 3-isocyanatopropyltriethoxysilane and **1** without any catalyst as reported earlier (Scheme 1).[30] This type of reaction is governed primarily by the basicity or nucleophilicity of amines. It involves the attack of electrophilic isocyanate group at the nucleophilic amino group of **1** having active hydrogen. The non-symmetric urea-substituted silatranes **3** and **4** were prepared by the transesterification reaction of **2** with triethanolamine and trisisopropanolamine, respectively.

Traditionally, the Michael addition reaction is catalysed by quantitative amount of strong bases and acids in conventional organic solvents which often leads to undesirable side reactions. To successfully catalyse the aza-Michael addition, other methods such as use of Lewis acids, ionic liquids, silica-supported catalysts and water as solvent have also been utilized for this transformation. In the present case, Michael donors and acceptors react via aza-Michael addition reaction under mild conditions which leads to the synthesis of Michael adduct azobenzene-substituted aminosuccinimide silatranes **8** and **9** as depicted in Scheme 2. In this reaction, aminopropylsilatranes **5** and **6** possessing NH_2 as nucleophilic group behave as Michael donors and **7** acts as Michael acceptor. Since **5** and **6** can act as both nucleophiles and bases, no additional base is typically required in this reaction.

Spectroscopic studies

The FT-IR spectra of all compounds were recorded as neat spectra in the range 400–4000 cm^{-1}. All silatranes (**3**, **4**, **8** and **9**) exhibit characteristic absorption bands of silatranyl group which are assigned on the basis of the literature.[31] The prominent contribution from the transannular N→Si bond is evident in the 550–590 cm^{-1} region. The absorption bands in the region 1550–1600 cm^{-1} are assigned to N=N stretching of azo group. The stretching vibration bands of C=O are seen at 1645–1665 cm^{-1} which are relatively weak due to resonance involved in NHC(=O)NH group for compounds **2**, **3** and **4**. The FT-IR spectra of silatranes **8** and **9** containing C=O functionality exhibit a typical absorption band at 1710 cm^{-1}. The absorption bands at 2800–2950 and 1600–1615 cm^{-1} correspond to methylene stretching and aromatic C=C bending, respectively. The absorption bands at 3300–3350 cm^{-1} are observed due to symmetric and asymmetric NH stretching for all compounds which supports the synthesis of desired compounds.

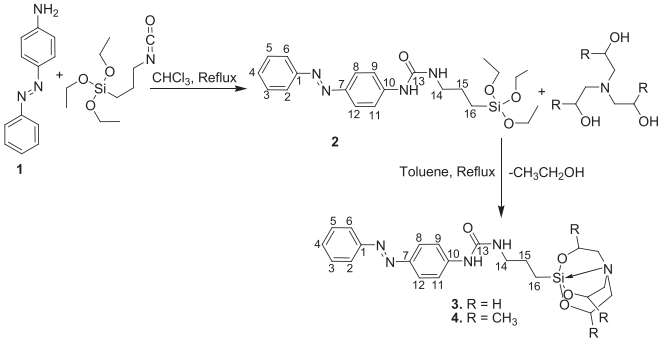

Scheme 1. Synthesis of azobenzene-substituted urea silatranes.

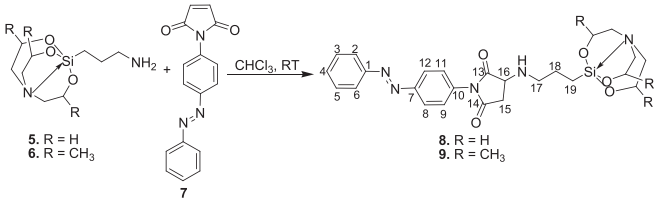

Scheme 2. Synthesis of azobenzene-substituted aminosuccinimide silatranes.

The NMR (^1H and ^{13}C) spectroscopic data were recorded for all compounds at room temperature and are found to accord with the structure of the synthesized products. In ^1H NMR spectra, the ethoxy group in silane **2** is replaced by atranyl moiety which is revealed by the appearance of two triplets due to NCH_2 (2.72 ppm) and OCH_2 (3.68 ppm) protons for compound **3**. As a result of three stereogenic CH_2CHMe carbon atoms, the ^1H NMR spectrum of compound **4** shows complex resonances and hints at the sample actually measured being composed of different diastereomers. The methylene protons (CH_2) are diastereotopic and they undergo geminal as well as vicinal coupling with methine proton (CH). Similar trends in chemical shifts are observed for atranyl moiety in the case of compounds **8** and **9**. Noteworthy, CH_2NH protons are validated by multiplets in the range 3.19–3.64 ppm for compounds **2**, **3** and **4** and in the range 2.64–2.66 ppm for compounds **8** and **9** depending upon exocyclic group attached to the silatrane. The rearrangement reaction for azobenzene-substituted urea silatranes is confirmed by the appearance of a broad singlet signal due to NH proton adjacent to propyl group in the region of 5.35–6.87 ppm for the compounds **2**, **3** and **4**. For these compounds, the signal of the other NH proton attached to azobenzene appears downfield at 7.09–7.68 ppm. The olefinic protons of **7** are observed as a singlet at 6.81 ppm. The aza-Michael addition reaction is indicated by the disappearance of these olefinic proton signals, which confirms Michael adduct formation. Both silatranes **8** and **9** exhibit a broad singlet for NH proton at 2.16 and 2.21 ppm, respectively. In ^{13}C NMR spectra, methylene carbon of CH_2Si appears as the most shielded carbon signal at 7.82 ppm for silane **2**. However, in the case of all silatranes, a downfield shift is observed for the same carbon. The aza-Michael reaction is confirmed by the appearance of an upfield methylene carbon signal for succinimide carbon at 36.66 and 36.64 ppm for silatranes **8** and **9**, respectively. The carbonyl carbons appear as the most downfield signal in the region of 155.38–158.63 ppm for compounds **2**, **3** and **4** and in the region of 170.50–176.67 ppm for compounds **8** and **9**.

The mass spectra of all the compounds (**2**, **3**, **4**, **8** and **9**) show the respective molecular ion peaks with the addition of H and possess characteristics silatrane fragmentation pattern. The peaks at *m/z* = 274 and 316 are observed due to the cleavage of azobenzene moiety which leads to the formation of *N*-propylsilatranylamide cation for compounds **3** and **4**, respectively. The mass spectra of compounds **8** and **9** also involve the formation of aminopropylsilatranyl cation moiety which appears at *m/z* = 233 and 248 for **8** and **9**, respectively. Besides these peaks, 1-propylsilatranyl ion (*m/z*: a = 216 (**3**, **8**), b = 233 (**4**, **9**)) peaks are also observed which lose one OCH (R)CH_2 arm to form bicyclic fragment with alkyl chain. The homolytic cleavage of Si–CH_2 leads to a silatranyl fragment with direct Si–N covalent bond (*m/z*: a = 174 (**3**, **8**), b = 216 (**4**, **9**)) that

corresponds to characteristic feature of mass spectrum of C-substituted silatrane involving the fragmentation of X–Si bond. This silatranyl fragment (*m/z*: a = 174 (**3**, **8**), b = 216 (**4**, **9**)) further loses a cyclic arm to form bicyclic moiety (*m/z*: a = 132 (**3**, **8**), b = 160). Very intense peaks due to protonated triethanolamine and trisisopropanolamine (*m/z*: a = 150 (**3**, **8**), b = 192 (**4**, **9**)) are also observed.

X-ray diffraction studies

Suitable crystals of **2** were eventually grown from tetrahydrofuran solvent at room temperature. The X-ray structure is presented in Fig. 1, and selected structural parameters are presented in Table 2 for compound **2**. The silicon-coordination polyhedra of **2** can be described as tetrahedral with all bond lengths and angles within the range of the expected values. The azobenzene group, which is the common part of the molecular skeleton of all studied compounds, is substantially planar in **2**. In the crystal, molecules are aligned on a twofold screw axis passing through the C10–O4 carbonyl group.

The hydrogen-bonding interactions, involving urea moieties (N2–H2···O4_$1, 2.862(2) Å, 155°; N1–H1···O4_$1, 2.959(2) Å 2.8, 150.3°; symmetry code $1 = $-x+1, -y-1, -z$) linked to adjacent molecules, generate a ribbon structure extending along the *b*-axis as described in Fig. 2. However along the *a*-axis, molecules are stacked via weak π–π interactions of 3.619(15) Å. π–π stacking interactions involve six-membered rings (C11–C12–C13–C14–C15–C16, $d_{centroid\text{-}centroid}$ = 3.6419(15) Å) which connect ribbons to build a two-dimeansional layer parallel to the *bc* plane. Both the interactions are weak however; the only possible interactions and playing a key role to form an overall three-dimensional lattice arrangement.

Compound **9** crystallizes in space group *C2/c* with one molecule in the asymmetric unit (Fig. 3(A)). The molecule has three stereo carbon centres (C2, C5 and C8) having absolute configurations of (*R*, *S*, *R*), respectively, and theoretically one would expect eight diastereomers. However, expanding all the eight molecules in the unit cells and with a close view along the *a*-axis it is found that half the molecules (four) are exactly inverted by the other half with completely opposite absolute configuration (*S*, *R*, *S*). Due to equal number of racemic mixtures (possible inversion of chiral centres during course of reaction),[32] the resulting space group (*C2/c*) is not a chiral one. Of the three asymmetric carbon centres, two atoms (C5, C8) and one nitrogen atom (N2) are disordered in two positions (Fig. 3(B)). Viewing the molecule along the N–Si axis, it looks like a molecular propeller having three propeller arms around the nitrogen centre (supporting information, Fig. S1b). The silicon atom in **9** exhibits a disordered trigonal bipyramidal coordination polyhedron with three equatorial sites occupied by oxygen atoms (O1, O2, O3) with two axial positons by carbon atom (C-10) and

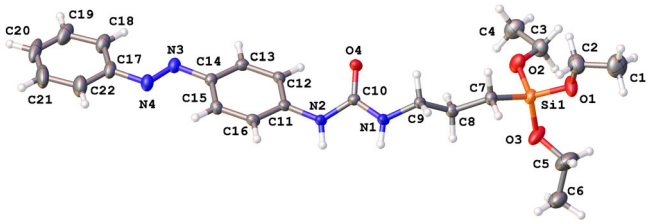

Figure 1. Molecular structure of **2** (probability level of displacement ellipsoids at 50%).

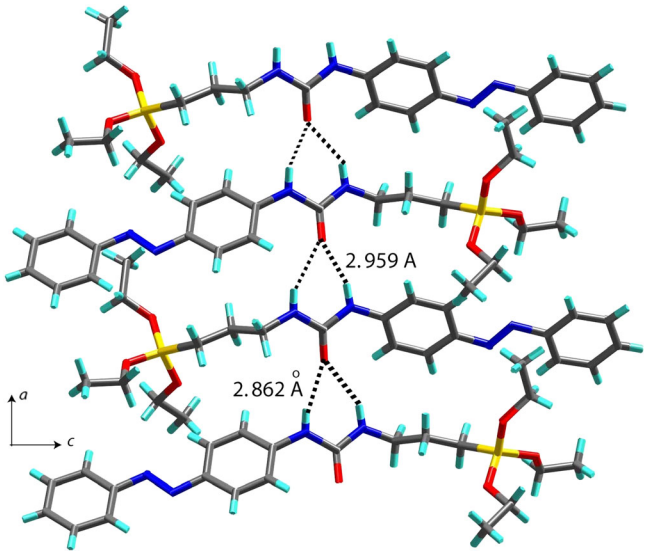

Figure 2. Molecular lattice arrangement for compound **2** along *b*-axis. Molecules are packed via weak hydrogen-bonding interactions between adjacent urea moieties of 2.959(2) and 2.862(2) Å.

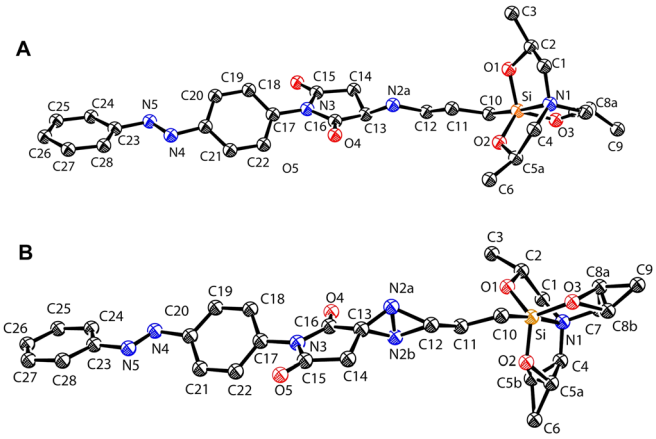

Figure 3. Molecular structure of **9** with probability of displacement ellipsoid at 50%. Hydrogen atoms are removed for clarity. (A) Molecule is depicted without including disordered atoms. (B) Molecule is depicted with disordered atoms for composition.

N1. The Addison parameter τ = 0.91 and Berry distortion of silicon-coordination polyhedral is 13.2% (O3 as the pivot atom). Unlike compound **2**, the azobenzene moiety in **9** adopts a non-coplanar arrangement (dihedral angles between phenyl rings are 37.21°). In compound **9**, two of the three arms of the trisisopropanolamine moiety are disordered over two positions showing different ratios of 0.44:0.56 (C5A:C5B) and 0.22:0.79 (C8A:C8B). Similarly, the disordered ratio at the N–H linker group of the aminopropylsilatrane moiety is 0.82:0.18 for N2A and N2B, respectively.

In the crystal lattice, antiparallel pairs of molecules (along *b*-axis) are associated by non-classical hydrogen-bonding interactions via methyl (C9) and succinimide (O5) groups as shown in Fig. 4(A). Though the hydrogen bonds are of non-classical type, these interactions (3.414 Å) are the only possible interactions and are of extremely weak type. Along the *a*-axis the three-dimensional pattern looks like an alternate layer-type arrangement of silatrane moiety and the rest of the alkyl chain (Fig. 4(B)). Again weak π–π

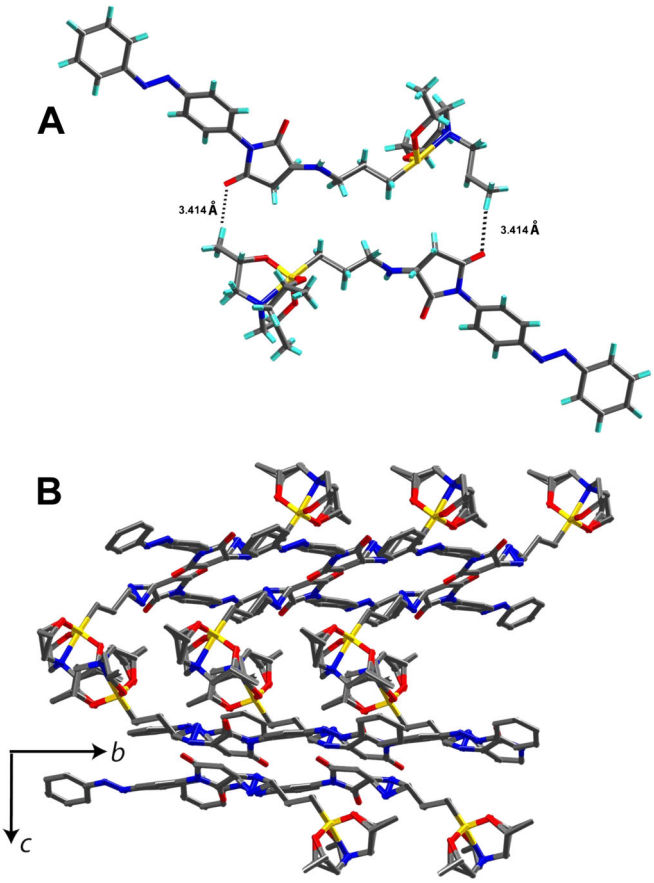

Figure 4. Molecular structure of **9** with packing and interactions. (A) Pair of molecules joined by non-classical interactions of methyl C9 and O5 with bond length of 2.416 Å. (B) Lattice arrangement of three-dimensional pattern along *a*-axis showing an alternate layer-type arrangement of silatrane moiety and the rest of the alkyl chain.

interactions between benzene rings (C17–C18–C19–C20–C21–C22, $d_{centriod\text{-}centriod} = 4.173$ Å) provide additional support for the three-dimensional arrangement.

Thermogravimetric analysis

The thermal stability of compounds **3**, **4**, **8** and **9** was studied using thermogravimetric analysis. All the compounds were heated from 25 to 1000°C under nitrogen atmosphere and isothermal conditions at a heating rate of 10°C min^{-1}. Additionally, thermogravimetric analysis is compared with the mass spectra and both analyses are found to be complementary to each other. For compounds **3** and **4**, three steps are observed, the first step involving the loss of 10.82 and 12.34%, respectively, due to ethanol and isopropanol formation. In the second step, cleavage of azobenzene group from **3** and **4** is observed from 200 to 350°C (calc. = 61.78, exp. = 61.48 (**3**) and calc. = 69.45, exp. = 69.58 (**4**)) which is further confirmed by mass spectral peaks at $m/z = 274$ and 316. Compounds **8** and **9** also display the same pattern for cleavage of azobenzene group. Compounds **8** and **9** show another step at 350–550°C (calc. = 35.84, exp. = 35.74 (**8**) and calc. = 32.84, exp. = 32.89 (**9**)) that corresponds to aminopropylsilatranyl moiety as residue which is complimentary with the mass spectra at $m/z = 233$ and 258, respectively. After annealing to 1000°C, SiO_2 residue formation is observed for all silatranes.

UV–visible studies

UV–visible titrations were performed with $(1–2) \times 10^{-5}$ M solutions of **3**, **4**, **8** and **9** in CH_3CN. Freshly prepared Bu_4NX ($X = Cl^-$, Br^-, I^- and CH_3COO^-) standard solutions were added and the UV–visible spectra of the samples were recorded. In UV–visible spectra, absorption peaks at 356 and 352 nm are observed for azobenzene-substituted urea silatranes **3** and **4** and azobenzene-substituted aminosuccinimide silatranes **8** and **9**, respectively, and these peaks are attributed to PhN=NPhNHC(=O)NH and $PhN{=}NPhN(CO)_2CH_2CHNH$ conjugated frameworks, respectively. The UV–visible spectra of all the silatranes change dramatically when a small amount of AcO^- ions are added, whereas no changes are observed upon the addition of Cl^-, Br^- and I^- ions up to 300 equiv. These silatrane-based receptors show strong binding to acetate over other ions such as Cl^-, Br^-, I^- and HSO_4^-. In the course of addition of AcO^- ions to silatrane **3**, the band around 356 nm is decreased and a bathochromic shift is observed passing through the isosbestic point at 403 nm as depicted in Fig. 5(A). The presence of the isosbestic point indicates that only two species are present at equilibrium over the course of the titration experiment.[33] The urea silatrane **3** moiety can be deprotonated due to the presence of more free acetate ions which can lead to the formation of highly stable anion species. The bathochromic shift may be observed due to an increase in conjugation between azobenzene group and deprotonated urea silatranes.[34,35] For azobenzene-substituted urea silatranes **3** and **4**, the same UV–visible spectral changes are observed in both silatranes due to their having the same axial

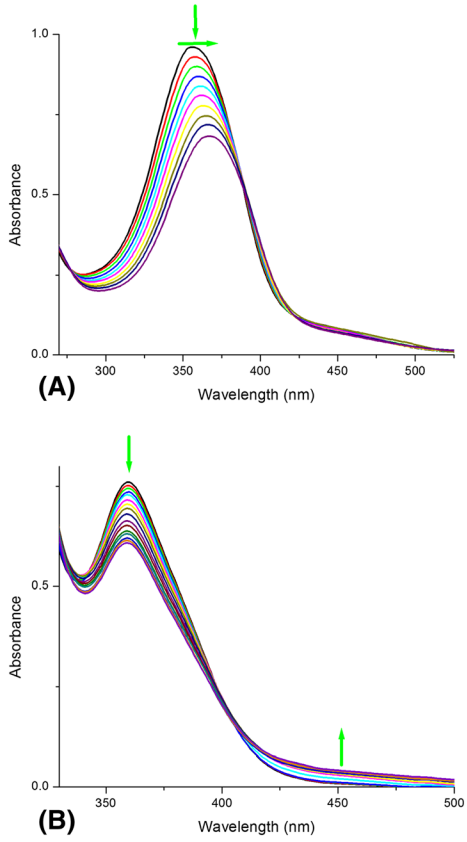

Figure 5. UV–visible spectral changes observed for **3** and **8** upon addition of acetate ions in CH_3CN at room temperature. (A) Compound **3** (1×10^{-5} M) with CH_3COO^- (0–10 equiv.) and (B) compound **8** (1.5×10^{-5} M) with CH_3COO^- (0–35 equiv.).

Table 3. MIC (mg ml^{-1}) of test compounds against reference strains

Microorganism	3	4	8	9
S. aureus ATCC 25923	0.20	0.40	>0.40	>0.40
A. baumannii ATCC 19606	0.20	0.40	>0.40	>0.40
P. aeruginosa ATCC 27853	0.20	0.20	>0.40	>0.40
E. coli ATCC 25922	0.20	0.40	>0.40	>0.40

group. This result indicates that there is no effect of substitution on UV–visible spectra of silatranes **3** and **4**. The UV–visible spectral changes of **3** and **4** with acetate ions are notably different from those of **8** and **9** with acetate ions. For azobenzene-substituted succinimide silatrane **8**, λ_{max} slowly moves from 352 to 363 nm along a hypochromic shift when 35 equiv. of acetate ions is added (Fig. 5(B)) which suggests the interaction of N–H of maleimide with acetate ions.

Biological activity

As a preliminary screening for antimicrobial activity, silatranes **3**, **4**, **8** and **9** are tested against bacterial strains of Gram-positive *Staphylococcus aureus* ATCC 25923 and Gram-negative *Acinetobacter baumannii* ATCC 19606, *Pseudomonas aeruginosa* ATCC 27853 and *Escherichia coli* ATCC 25922. The antimicrobial activity results of the silatranes tested are listed in Table 3. All of the silatranes (**3**, **4**, **8** and **9**) are found to have moderate antimicrobial activity against all test microorganisms. Among the four silatranes, **3** shows efficient MIC against all control bacteria. Silatrane **4** shows a significant MIC of 0.20 mg ml^{-1} against *P. aeruginosa* ATCC 27853 and 0.40 mg ml^{-1} against the other microorganisms. These results for compounds **3** and **4** may be attributed to the presence of urea group. Silatranes **8** and **9** show high MICs (>0.40 mg ml^{-1}) for both Gram-positive and Gram-negative bacteria which reveal less antimicrobial activity than urea-containing silatranes **3** and **4**. The results are compared with earlier reported antimicrobial studies using the broth microdilution method. The azo group-substituted silatranes show superior results compared to triethylammonium-3-silatranylpropyldithiocarbamate, which may be attributed to the substituted azo moiety.

Conclusions

New 4-aminoazobenzene-based silatranes bearing urea and aminosuccinimide groups as linker moieties at axial position of silatranes have been successfully synthesized in good yields. UV–visible spectra of azobenzene-substituted urea and aminosuccinimide silatranes have been studied. These linker groups make these silatranes solid candidates for supramolecular chemistry due to availability of binding sites. These hybrid inorganic–organic materials are promising systems for an array of applications due to their extraordinary properties based on the combination of the different building blocks. A preliminary biological evaluation has revealed potential antimicrobial activity possessed by the silatranes.

Acknowledgments

The authors are grateful to UGC, New Delhi for financial support.

References

[1] H. Zollinger, *Color Chemistry: Synthesis, Properties, and Applications of Organic Dyes and Pigments*, 2nd revised edn, VCH, Weinheim, **1991**.
[2] E. Ispir, *Dyes Pigm.* **2009**, *82*, 13.
[3] X. G. Wang, J. Kumar, S. K. Tripathy, L. Li, J. Chen, S. Marturunkakul, *Macromolecules* **1997**, *30*, 219.
[4] Y. Cui, M. Wang, L. Chen, G. Qian, *Dyes Pigm.* **2004**, *62*, 43.
[5] A. Natansohn, P. Rochon, *Chem. Rev.* **2002**, *102*, 4139.
[6] D. Wang, D. Xie, W. Shi, S. Sun, C. Zhao, *Langmuir* **2013**, *29*, 8311.
[7] M. E. Moustafa, M. S. McCready, R. J. Puddephatt, *Organometallics* **2012**, *31*, 6262.
[8] A. Dirksen, E. Zuidema, R. M. Williams, L. De Cola, C. Kauffmann, F. Vogtle, A. Roque, F. Pina, *Macromolecules* **2002**, *35*, 2743.
[9] H. G. Garg, R. A. Sharma, *J. Med. Chem.* **1996**, *12*, 1122.
[10] Y. M. Song, Y. M. Ha, J. A. Kim, K. W. Chung, Y. Uehar, K. J. Lee, P. Chun, Y. Byun, H. Y. Chung, H. R. Moon, *Bioorg. Med. Chem. Lett.* **2012**, *22*, 7451.
[11] G. Singh, A. Saroa, M. Garg, R. P. Sharma, A. I. Gubanov, A. I. Smolentsev, *J. Organometal. Chem.* **2012**, *719*, 21.
[12] B. J. Brennana, D. Gust, G. W. Brudviga, *Tetrahedron Lett.* **2014**, *55*, 1062.
[13] G. Singh, S. S. Mangat, J. Singh, A. Arora, M. Garg, *J. Organometal. Chem.* **2014**, *769*, 124.
[14] G. Singh, S. S. Mangat, H. Sharma, J. Singh, A. Arora, A. P. S. Pannu, N. Singh, *RSC Adv.* **2014**, *4*, 36834.
[15] J. J. E. Moreau, L. Vellutini, M. W. C. Man, C. Bied, *J. Am. Chem. Soc.* **2001**, *123*, 1509.
[16] Y. Cui, G. Qian, L. Chen, Z. Wang, M. Wang, *Thin Solid Films* **2008**, *516*, 5483.
[17] P. Charpentier, J. Briere, G. Dupas, G. Queguiner, J. Bourguignon, *Tetrahedron* **1996**, *52*, 10441.
[18] Y. Bi, L. Bailly, F. Marsais, V. Levacher, C. Papamicael, G. Dupas, *Tetrahedron Asymmetry* **2004**, *15*, 3703.
[19] P. Tharmaraj, D. Kodimunthiriy, C. D. Sheelaz, C. S. Priya, *J. Coord. Chem.* **2009**, *62*, 220.
[20] H. Huang, J. Jian, Y. Lee, Y. Li, T. Huang, J. Chang, L. Yeh, J. Yeh, *Polymer* **2012**, *53*, 4967.
[21] A. Dumitriu, M. Cazacu, S. Shova, C. Tturta, B. C. Simionescu, *Polyhedron* **2012**, *33*, 119.
[22] X. Xue, J. Zhu, Z. Zhang, N. Zhou, X. Zhu, *React. Funct. Polym.* **2010**, *70*, 456.
[23] Bruker, *APEX2 software, V.2013.6*, Bruker AXS Inc., Madison, WI, USA, **2013**.
[24] G. M. Sheldrick, *SADABS, Program for Empirical Absorption Correction of Area Detector Data*, University of Göttingen, Germany, **2009**.
[25] G. M. Sheldrick, *Acta Crystallogr. A* **2008**, *A64*, 112.
[26] A. L. Spek, PLATON, *A Multipurpose Crystallographic Tool*, Utrecht University, Utrecht, The Netherlands, **2010**.
[27] O. V. Dolomanov, L. J. Bourhis, R. J. Gildea, J. A. K. Howard, H. J. Puschmann, *J. Appl. Crystallogr.* **2009**, *42*, 339.
[28] C. F. Macrae, I. J. Bruno, J. A. Chisholm, P. R. Edgington, P. McCabe, E. Pidcock, L. Rodriguez-Monge, R. Taylor, J. van de Streek, P. A. Wood, *J. Appl. Crystallogr.* **2008**, *41*, 466.
[29] I. Wiegand, K. Hilpert, R. E. W. Hancock, *Nat. Protoc.* **2008**, *3*, 163.
[30] S. R. Sandler, W. Karo, *Organic Functional Group Preparations*, *Vol. 2*, Academic Press, New York, **1971**, pp. 135.
[31] M. Imbernotte, G. Palavit, P. Legrand, J. P. Huvenne, G. Fleury, *J. Mol. Spectrosc.* **1983**, *102*, 40.
[32] A. Streitwieser, C. H. Heathcock, *Introduction to Organic Chemistry*, 3rd edn, Maxwell MacMillan, New York, **1985**, pp. 122.
[33] V. Amendola, D. Estenban-Gómez, L. Fabbrizzi, M. Liccgelli, *Acc. Chem. Res.* **2006**, *39*, 343.
[34] Y. Kim, H. Kwak, S. J. Lee, J. S. Lee, H. J. Kwon, S. H. Nam, K. Lee, C. Kim, *Tetrahedron* **2006**, *62*, 9635.
[35] C. R. Bondy, S. J. Loeb, *Coord. Chem. Rev.* **2003**, *240*, 77.

Supporting information

Additional supporting information may be found in the online version of this article at the publisher's web-site.